Supplemental Figure 1. Structural formula of the copper(II) bis(thiosemicarbazone) complexes, Cu-PTSM ($R_1 = R_2 = CH_3$) and Cu-ETS ($R_1 = -CH_2CH_3$, $R_2 = H$). "H_2PTSM" is the acronym for pyruvaldehyde bis(N[4]-methyl-thiosemicarbazone), and "H_2ETS" is ethylglyoxal bis(thiosemicarbazone). These uncharged, lipophilic chelates have shown promise for use as [62]Cu-radiopharmaceuticals for PET perfusion imaging with PET (1-21). In addition to exhibiting the desired high first-pass tissue extraction of tracer, these agents also desirably afford prolonged "microsphere-like" tissue retention of the radiolabel (5,12,20,21), as they undergo rapid intracellular reductive decomposition liberating ionic [62]Cu into the endogenous intracellular copper pool (20-24). Contrary to findings in animal models (6,7,8,21), in *humans* Cu-PTSM tends to underestimate the rate of perfusion in high flow tissues (9,10,13), because it exhibits a high, species-specific, affinity for the IIA Warfarin-binding site of human serum albumin (25-27) that limits its otherwise efficient first-pass extraction into tissue at high flow rates. This high-affinity interaction with HSA does not appear feasible when the pyruvaldehyde methyl group is replaced with bulkier ethyl group of the Cu-ETS chelate (27), making Cu-ETS the preferred choice for imaging perfusion in the human tissues that can have high rates of perfusion, such as the heart, kidney, and some tumors.

In Vitro Assay to Define the Kinetics of [[62]Cu]Cu-ETS Decomposition by Patient Blood.

Because a portion of the injected [[62]Cu]Cu-ETS radiopharmaceutical will be reductively decomposed by the patient's blood cells, in vitro assays were performed to directly examine the rate of [[62]Cu]Cu-ETS decomposition in patient blood (28), allowing correction of the PET-derived arterial blood [62]Cu time-activity curve to represent the fraction of blood radioactivity expected to remain present as intact [[62]Cu]Cu-ETS.

Prior to PET imaging, a 1-mL sample of the patient's blood was collected into a heparinized syringe, and transferred to a polypropylene centrifuge tube in a thermomixer for maintenance at 37°C with gentle swirling (300 rpm). A 50-µL sample of the [[62]Cu]Cu-ETS product solution was added to the blood sample. At 10, 20, 30, 40, 50, 60, 90, 120, 180, 240, and 300-seconds post-mixing, 25-µL samples of the [62]Cu-blood were transferred to centrifuge tubes containing 1000-

µL *n*-octanol, vortex mixed, and then centrifuged at 10,000 x G for 5-minutes. The octanol and cell debris pellet were separated, and the samples counted in a NaI(Tl) well-counter to quantify the fraction of the blood [62]Cu remaining present as octanol-soluble [[62]Cu]Cu-ETS (8,9,12,28).

The rate of [[62]Cu]Cu-ETS decomposition by blood was always a first-order process. However, that rate showed considerable variability between subjects (Supplemental Figure 2), as well as between the baseline and during-treatment studies of an individual subject. The average rate of [[62]Cu]Cu-ETS decomposition by human blood (Supplemental Figure 2) was somewhat faster than what we previously observed with porcine blood (12).

The plotted equation is:

$$y = -0.0072x + 4.0$$
$$R^2 = 0.64$$
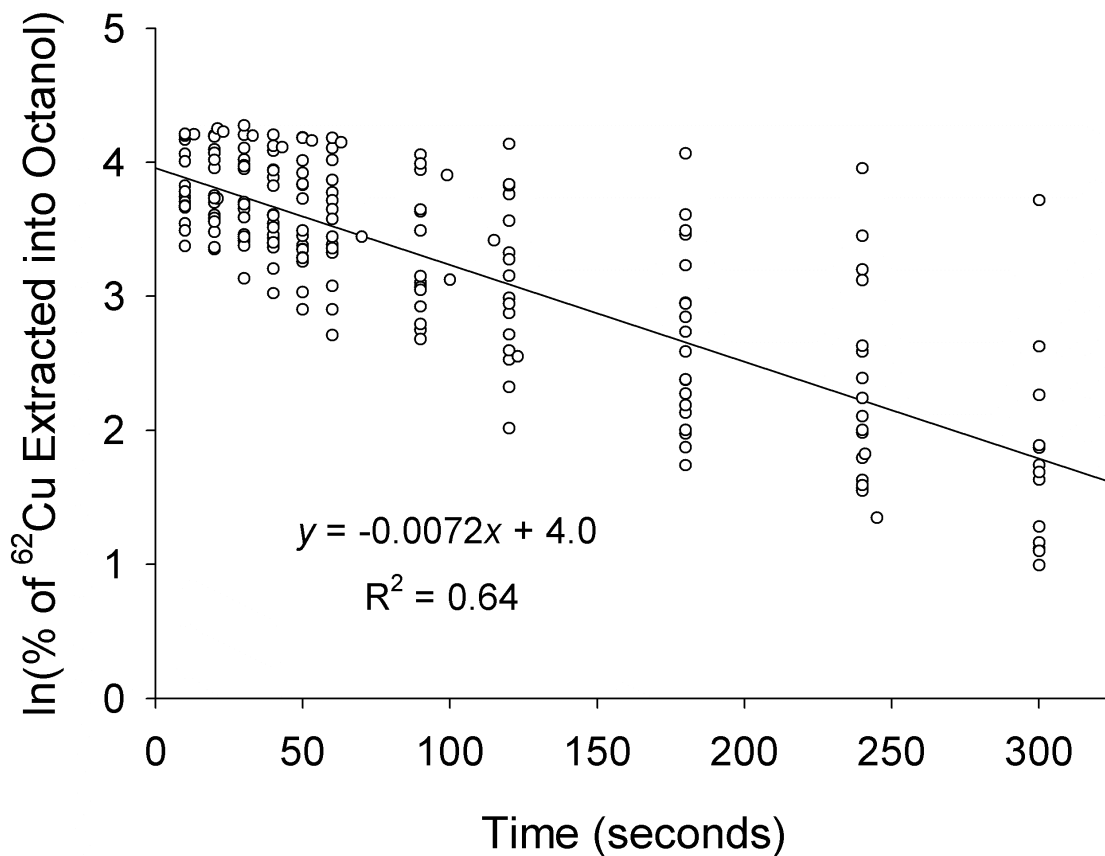
Supplemental Figure 2. Decomposition of [[62]Cu]Cu-ETS by human blood in vitro at 37°C.

Radiation Dosimetry

Radiation dosimetry estimates for the [^{62}Cu]Cu-ETS radiopharmaceutical are available from the Proportional Technologies, Inc. ^{62}Cu-ethylglyoxal (bis(thiosemicarbazone) Investigator's Brochure:

http://www.proportionaltech.com/new_site/images/stories/Investigator_Brochure_ETS.pdf

The whole body effective dose equivalent for [^{62}Cu]Cu-ETS is 9.47×10^{-3} mSv/MBq (35 mrem/mCi) (male) and 1.14×10^{-2} mSv/MBq (42 mrem/mCi) (female). The kidneys are expected to be the critical organ, receiving an estimated 3.90×10^{-2} mSv/MBq (144 mrem/mCi) (male) and 4.24×10^{-2} mSv/MBq (157 mrem/mCi) (female).

PET/CT Data Analysis

The standard two-compartment model routinely employed for the measurement of blood flow in the brain and heart was applied to the measurement of tumor perfusion with ^{15}O-water (30-38). In this model, the transport of the tracer from the vasculature to the interstitial space is assumed to be sufficiently rapid that the single-pass extraction fraction of water is approximately equal to 1.0 across the range of perfusion values. This model consists of two rate constants, K_1 and k_2, representing the tissue perfusion and tracer washout rates, respectively. Both model rate constants are related to tissue perfusion with:

$$K_1 = \text{RBF} \times \text{EF} \quad k_2 = \text{RBF} / V_d.$$

In these equations *RBF* is regional blood flow, *EF* is the tracer single pass extraction fraction, and V_d is the tracer volume of distribution in tissue. In order to maintain consistency between the estimation of RBF using ^{15}O-Water and ^{62}Cu-ETS, we used K_1 as our perfusion estimate.

Correction of the measured data for factors resulting from the limited image resolution achievable from current generation PET imaging systems (detector geometry as well as respiratory motion) is necessary for the absolute quantification of physiologic processes. An approach previously developed and validated for myocardial PET imaging applications was utilized to minimize the bias caused by these resolution-based distortions (32). Attention was paid in the definition of tumor regions-of-interest to assure that the assumption is met that the data can be described by a linear combination of tumor tissue activity and blood pool activity. These methods were implemented by modifying the mathematical expressions describing the radionuclide concentration in a region-of-interest as follows:

$$C_{voi}(t) = (1-F_{BV})C_T(t) + F_{BV}C_a(t)$$

where $C_{roi}(t)$ is the measured region-of-interest concentration, $C_T(t)$ is the tumor tissue concentration, $C_a(t)$ is the arterial blood concentration, and F_a is the fraction of the region-of-interest volume occupied by arterial blood.

For tumors in the lungs, it was necessary to define the source of arterial blood flow to each lesion by analysis of the tumor radioactivity time-activity curve relative to the time-activity curves for regions in the blood pool of the right ventricle and left atrium. If blood counts from the intravenously administered radiopharmaceutical arrived at the tumor prior to tracer appearance in the left atrium, the right ventricular blood ROI was used for defining that tumor's arterial input. Otherwise, tumor blood flow, and that of the thyroid, myocardium, and muscle reference tissues, was modeled with the arterial input function derived from the blood pool of the left atrium.

For [62]Cu-ETS PET, flow was quantified using a 2-compartment model that was previously used with success in myocardial flow quantification with [62]Cu-PTSM in the dog (6,8). In our implementation of this model, the transport of tracer from the vasculature through the interstitial space and into the cellular compartment is assumed sufficiently rapid that the delivery rate is perfusion limited. Once in the cellular compartment, tracer is retained by the cell ($k_2 = 0$). The tracer concentration within a defined volume of interest $C_{VOI}(t)$ can then be defined as a function of the arterial blood concentration, $C_a(t)$, by:

$$C_{VOI}(t) = \frac{(1 - f_{BV})}{(t_2 - t_1)}\int_{t_1}^{t_2} C_T(\tau)d\tau + \frac{f_{BV}}{(t_2 - t_1)}\int_{t_1}^{t_2} C_A(\tau)d\tau$$

$$C_T(t) = K_1 \int_{t_1}^{t_2} C_A^*(\tau)d\tau$$

$$K_1 = F \times EF = F(1 - e^{-PS/F})$$

Where F = tissue perfusion (mL/min/g), EF = extraction fraction, PS = permeability – surface area product, $C_A(t)$ = [62]Cu concentration in arterial blood, $C_A^*(t)$ = [62]Cu-ETS concentration in arterial blood, fBV = fraction of the volume of interest volume occupied by arterial blood, and t_1, t_2 are the start and stop times of each image frame.

The model was fit using the arterial blood concentration of [62]Cu to define the input function for PET quantification of tumor and normal tissue blood flow, defining the arterial input function from the data provided by a volume-of-interest positioned on the blood pool of the left atrium (or right ventricle for some lung lesions). The raw arterial blood [62]Cu time-activity curve ($C_A(t)$)was corrected to the [62]Cu-ETS time-activity curve ($C_A^*(t)$) by applying the measured rate of [62]Cu-ETS decomposition in the patient's blood at 37°C.

Positron Range Considerations

Copper-62 emits positrons at higher energy than oxygen-15, which will somewhat impact spatial resolution in ^{62}Cu *vs.* ^{15}O PET images. The potential impact associated with positron range upon the observed lesion signal includes: *(i)* a reduction in the observed ^{62}Cu concentration in an isolated lesion, due to the long positron range in low density tissue adjacent to that lesion; and *(ii)* an increase in observed ^{62}Cu concentration in the isolated lesion, due to positrons originating in surrounding tissue annihilating within the more dense lesion volume. The relative impact of these competing processes will depend upon lesion size, surrounding tissue density, and the lesion-to-background ^{62}Cu concentration ratio. The potential limitations that may be caused by the ^{62}Cu positron range include: *(i)* large underestimation of perfusion in small lesions, and loss of ability to detect these lesions over background; and *(ii)* overestimation of perfusion in low perfusion lesions, particularly if there is tracer uptake in surrounding low density tissue, or in scenarios in which background uptake exceeds lesion uptake. Nonetheless, the correlations we observed between ^{62}Cu-ETS and ^{15}O water perfusion estimates are strong (Figures 4 and 5) and there were no lesions observed with ^{15}O-water that were not observed with ^{62}Cu-ETS, or vise versa. Theoretically one could implement a positron range correction in the reconstruction algorithm, but it is unclear that this would provide a benefit from a clinical perspective.

REFERENCES FOR SUPPLEMENTAL DATA

1. M.A. Green, The potential for generator-based PET perfusion tracers. *J. Nucl. Med.* 31:1641-1645, 1993.

2. M.A. Green, C.J. Mathias, M.J. Welch, A.H. McGuire, D. Perry, F. Fernandez-Rubio, J.S. Perlmutter, M.E.Raichle, and Bergmann S.R., [[62]Cu]-labeled pyruvaldehyde *bis*(*N*[4]-methylthiosemicarbazonato)copper(II): synthesis and evaluation as a positron emission tomography tracer for cerebral and myocardial perfusion. *J. Nucl. Med.* 31:1989-1996, 1990.

3. N.G. Haynes, J.L. Lacy, N. Nayak, C.S. Martin, D. Dai, C.J. Mathias, and M.A. Green, Performance of a Zn-62/Cu-62 generator in clinical trials of the perfusion agent Cu-62-PTSM. J. Nucl. Med. 41:309-314; 2000.

4. T.R. Wallhaus, J. Lacy, J. Whang, M.A. Green, R.J. Nickles, C.K. Stone. Human biodistribution and dosimetry of the PET perfusion agent copper-62-PTSM from a compact modular 62Zn/62Cu generator system. *J. Nucl. Med. 39:*1958-1964; 1998.

5. E. John and M.A. Green, Structure-activity relationships for metal-labeled blood flow tracers: comparison of ketoaldehyde *bis*(thiosemicarbazonato)copper(II) derivatives. *J. Med. Chem.*, 33:1764-1770, 1990.

6. M.E. Shelton, M.A. Green, C.J. Mathias, M.J. Welch and S.R. Bergmann, Assessment of regional myocardial and renal blood flow using copper-PTSM and positron emission tomography. *Circulation* 82:990-997, 1990.

7. C.J. Mathias, M.A. Green, W.B. Morrison, and D.W. Knapp, Evaluation of Cu-PTSM as a tracer of tumor perfusion: comparison with labeled microspheres in spontaneous canine neoplasms, *Nucl. Med. Biol.*, 21:83-87; 1994.

8. P. Herrero, J. Markham, C.J. Weinheimer, C.J. Anderson, M.J. Welch, M.A. Green, and S.R. Bergmann, Quantification of regional myocardial perfusion with generator-produced 62Cu-PTSM and positron emission tomography. *Circulation* 87:173-183, 1993.

9. P. Herrero, J.J. Hartman, M.A. Green, C.J. Anderson, M.J. Welch, J. Markham, and S.R. Bergmann, Assessment of Regional Myocardial Perfusion with Generator-Produced 62Cu-PTSM and PET in Human Subjects. *Journal of Nuclear Medicine,* 37:1294-1300; 1996.

10. T.R. Wallhaus, J. Lacy, R. Stewart, J. Bianco, M.A. Green, and C.K. Stone. Copper-62-pyruvaldehyde bis(N4-methylthiosemicarbazone) PET imaging in the Detection of Coronary Artery Disease in Humans, J. Nucl. Cardiol. 8:67-74; 2001.

11. C.J. Mathias, M.J.Welch, D.J. Perry, A.H. McGuire, X. Zhu, J.M. Connett, and M.A. Green. Investigation of copper-PTSM as a PET tracer for tumor blood flow. Nucl. Med. Biol. 18:807-811; 1991.

12. M.A. Green, C.J. Mathias, L.R. Willis, R.K. Handa, J.L. Lacy, M.A. Miller, G.D. Hutchins, Assessment of Cu-ETS as a PET radiopharmaceutical for evaluation of regional renal

perfusion. Nucl Med Biol. 34:247-255; 2007.

13. R. S. Beanlands, O. Muzik, M. A. Mintun, T. Mangner, K. Lee, N. Petry, G. D. Hutchins, M. Schwaiger, The kinetics of copper-62-PTSM in the normal human heart. *J. Nucl. Med.* 33:684-690, 1992.

14. P.G. Melon, C. Brihaye, C. Degueldre, M. Guillaume, R. Czichosz, P. Rigo, H. Kulbertus, D. Comar, Myocardial kinetics of K-38 in humans and comparison with Cu-62-PTSM, *J. Nucl. Med., 35,* 1116-1122,1994.

15. R.S.B. Beanlands, O. Muzik, G.D. Hutchins, E.R. Woulfe, and M. Schwaiger, Heterogeneity of regional nitrogen-13-labeled ammonia tracer distribution in the normal human heart: comparison with rubidium-82 and copper-62-labeled PTSM. J. Nucl. Cardiol. 1:225-235; 1994.

16. H. Okazawa, Y. Yonekura, Y. Fujibayashi, et al., Clinical application and quantitative evaluation of generator-produced copper-62-PTSM as a brain perfusion tracer for PET, J. Nucl. Med. 35:1910-1915; 1994.

17. Tadamura E, Tamaki N, Okazawa H, Fujibayashi Y, Kudoh T, Yonekura Y, Magata Y, Nohara R, Sasayama S, Konishi J, Generator-produced copper-62-PTSM as a myocardial PET perfusion tracercompared with nitrogen-13-ammonia. J. Nucl. Med. 37:729-735; 1996.

18. Okazawa H, Yonekura Y, Fujibayashi Y, Nishizawa S, Magata Y, Ishizu K, Tanaka F, Tsuchida T, Tamaki N, Konishi J, Clinical application and quantitative evaluation of generator-produced copper-62-PTSM as a brain perfusion tracer for PET. J. Nucl. Med. 35:1910-1915; 1994.

19. Okazawa H, Yonekura Y, Fujibayashi Y, Mukai T, Nishizawa S, Magata Y, Ishizu K, Tamaki N, Konishi J. Measurement of regional cerebral blood flow with copper-62-PTSM and a three-compartment model. J. Nucl. Med. 37:1089-1093; 1996.

20. M.E. Shelton, M.A. Green, C.J. Mathias, M.J. Welch, S.R. Bergmann, Kinetics of copper-PTSM in isolated hearts: a novel tracer for measuring blood flow with positron emission tomography. *J. Nucl. Med.,* 30:1843-1847, 1989.

21. C.J. Mathias, M.J. Welch, M.E. Raichle, M.A. Mintun, L.L. Lich, A.H. McGuire, K.R. Zinn, E.K. John and M.A. Green, Evaluation of a potential generator-produced PET tracer for cerebral perfusion imaging: single-pass cerebral extraction measurements and imaging with radiolabeled Cu-PTSM. *J. Nucl. Med.* 31:351-359, 1990.

22. D.T. Minkel, L.A. Saryan, and D.H. Petering, Structure-function correlations in the reaction of *bis*(thiosemicarbazone) copper(II) complexes with Ehrlich acites tumor cells. *Cancer Res.* 38:124-129, 1978.

23. D.A. Winkelmann, Y. Bermke, D.H. Petering, Comparative properties of the antineoplastic agent 3-ethoxy-2-oxobutyraldehyde *bis*(thiosemicarbazone) copper(II) and related chelates: linear free energy relationships. *Bioinorg. Chem.* 3:261-277, 1974.

24. Baerga ID, Maickel RP & Green MA, Subcellular Distribution of Tissue Radiocopper

Following Intravenous Administration of 67Cu-labeled Cu-PTSM. Nucl. Med. Biol., 19, 697-701; 1992.

25. C.J. Mathias, S.R. Bergmann, and M.A. Green, Species-dependent binding of copper(II) bis(thiosemicarbazone) complexes to serum albumin. *J. Nucl. Med*. 36:1451-1456; 1995.

26. N.E. Basken, C.J. Mathias, and M.A. Green. Elucidation of the Human Serum Albumin (HSA) Binding Site for the Cu-PTSM and Cu-ATSM Radiopharmaceuticals, J Pharm Sci., 98:2170-2179; 2009.

27. N.E. Basken, and M.A. Green. Cu(II) Bis(thiosemicarbazone) Radiopharmaceutical Binding to Serum Albumin: Further Definition of Species-Dependence and Associated Substituent Effects, Nucl Med Biol, 36:495-504; 2009.

28. C.J. Mathias, S.R. Bergmann and M.A Green, Development and validation of a solvent extraction technique for determination of Cu-PTSM in blood. *Nucl. Med. Biol.,* 20:343-349, 1993.

29. Bergmann SR, Fox KA, Rand AL, et al. Quantification of regional myocardial blood flow in vivo with $H_2{}^{15}O$. *Circulation*. 1984;70:724–733.

30. Huang S-C, Schwaiger M, Carson RE, et al. Quantitative measurement of myocardial blood flow with oxygen-15 water and positron computed tomography: an assessment of potential and problems. *J Nucl Med*. 1985;26:616–625.

31. Herrero P, Markham J, Bergmann SR. Quantitation of myocardial blood-flow with (H2O)-O-15 and positron emission tomography—assessment and error analysis of a mathematical approach. *J. Comput. Assist. Tomog*. 1989;13:862–873.

32. Hutchins GD, Caraher J, Raylman RR. A Region of Interest Strategy for Minimizing Resolution Distortions in Quantitative Myocardial PET Studies. *J Nucl Med* 1992;33:1243-1250.

33. Frackowiak RSJ, Lenzi G-L, Jones T, Heather JD. Quantitative measurement of regional cerebral blood flow and oxygen metabolism in man using O-15 and positron emission tomography: theory, procedure, and normal values. *J Comput Assist Tomogr*. 1980;4:727-736.

34. Herscovitch P, Markham J, Raichle ME. Brain blood flow measured with intravenous $H_2{}^{15}O$. I. Theory and error analysis. *J Nucl Med*. 1983;24:782–789.

35. Bacharach SL, Libutti SK, Carrasquillo JA, Measuring tumor blood flow with $H_2{}^{15}O$: practical considerations. *Nucl Med Biol*. 2000;27:671-676.

36. Lodge MA, Carson RE, J.A. Carrasquillo JA, Whatley M, Libutti SK, Bacharach SL, Parametric images of blood flow in oncology PET studies using [^{15}O]water. *J Nucl Med*. 2000;41:1784-1792.

37. Lehtiö K, Eskola O, Viljanen T, et al. Imaging perfusion and hypoxia with PET to predict radiotherapy response in head-and-neck cancer. *Int. J. Radiation Oncology Biol. Phys*. 2004;59:971-982.

Page 8 of 9

THE JOURNAL OF NUCLEAR MEDICINE • Vol. 56 • No. 1 • January 2015 Fletcher et al.

38. Logan TF, Jadali F, Egorin MJ, et al. Decreased tumor blood flow as measured by positron emission tomography in cancer patients treated with interleukin-1 and carboplatin on a phase I trial. *Cancer Chemotherapy and Pharmacology* 2002;50:433-444.